



## Fuel cell electrodes using carbon nanostructures

M. Lebert<sup>a,\*</sup>, M. Kaempgen<sup>b</sup>, M. Soehn<sup>c</sup>, T. Wirth<sup>d</sup>, S. Roth<sup>a</sup>, N. Nicoloso<sup>c</sup>

<sup>a</sup> Max-Planck-Institute for Solid State Research, D-70569 Stuttgart, Germany

<sup>b</sup> University of California, Department of Physics and Astronomy, Los Angeles, CA, USA

<sup>c</sup> TU Darmstadt, Department of Renewable Energies, D-64283 Darmstadt, Germany

<sup>d</sup> University of Cambridge, Department of Engineering, Cambridge CB2 1PZ, UK

### ARTICLE INFO

#### Article history:

Available online 23 December 2008

#### Keywords:

Carbon nanotubes  
Fuel cell  
GDE  
HT-PEMFC  
PAFC  
PEMFC  
SWNT  
MWNT

### ABSTRACT

The use of carbon nanotubes (SWNT, MWNT, and aligned CNT) for low and intermediate temperature fuel cells has been investigated with thin film CNT/Pt-electrodes of ( $1 < d < 10 \mu\text{m}$ ). For membrane electrode assembly (MEA) the electrodes were combined either with Nafion<sup>®</sup> 117 or polycarbonate (PC) membranes wetted with  $\text{H}_3\text{PO}_4$ . The fuel cell characteristics of the CNT-based MEAs were determined at atmospheric pressure, different catalyst concentrations (Pt) and temperatures ( $\text{RT} < T < 150^\circ\text{C}$ ). The performance is competitive to well-established phosphoric acid (PAFCs) or polymer electrolyte membrane fuel cell (PEMFC), e.g. PBI/ $\text{H}_3\text{PO}_4$ . Liquid state processing of CNTs allows flexible electrode design and opens new ways for integrated and significantly mass-/volume-reduced fuel cell electrodes with high saving potential for catalyst and carbon material. Microsized high performance power supplies and battery chargers for consumer electronics are the most promising applications.

© 2008 Elsevier B.V. All rights reserved.

## 1. Introduction

A great deal of research is currently performed on fuel cells (FC) as energy conversion devices with hydrogen and C1 (or higher) compounds as fuels. Due to efficiency advantages they are an interesting alternative to combustion engines, especially in the low temperature range ( $T < 200^\circ\text{C}$ ). To achieve further improvement in performance and long-term stability materials, designs and production techniques have to be established, however. Carbon nanotubes (CNTs) have raised many expectations due to their unique properties, e.g. high (electro)chemical stability, high electrical conductivity and high surface area. Randomly oriented single or multiwalled carbon nanotubes (SWNTs, MWNTs) can be easily converted into highly conducting thin porous networks suitable for gas diffusion electrodes (GDEs) in FCs [1,2]. Partially aligned MWNTs grown on commercial carbon fibres [3] combine the well known properties of conventional carbon electrodes with the high specific surface area of MWNTs (up to  $1000 \text{ m}^2/\text{g}$  [4]). Fully aligned nanocarbon materials can be prepared by the vertical growth of MWNTs on thermally insulating substrates allowing well-defined spatial distribution of properties. Aligned MWNTs are discussed as gas diffusion layers [5,6] and catalyst support [7,8].

The materials essentially differ with respect to the local structure and surface area and thus the actual state of the three-phase boundary catalyst/reactant gas/electrolyte. As main advantage CNTs allow flexible electrode design and processing, especially suited for small-scale applications, e.g. nano/micro-sized FCs with high power density.

## 2. Experimental

Carbon nanostructures with different ordering and morphology have been prepared as catalyst supports and tested in a home made fuel cell test bench at  $\text{RT} < T < 150^\circ\text{C}$  under atmospheric pressure in PAFC and PEMFC configuration. In the following the main experimental results are presented.

### 2.1. Random, non-aligned CNT network electrodes

#### 2.1.1. SWNT network electrodes

SWNTs made by high pressure CO disproportionation (HiPco [9,10]) from CNI/Unidym<sup>®</sup> are purified and functionalized by ultrasonication in conc.  $\text{HNO}_3$  as reported in detail elsewhere [11]. Briefly, the oxidative treatment introduces oxygen surface defects ( $-\text{OH}$ ,  $-\text{C}=\text{O}$ ,  $-\text{COOH}$  [1]) into the SWNT thereby enhancing their solubility in aqueous solutions and their conductivity [12]. In order to achieve a thin monolithic GDE with a hydrophobic gas diffusion part and a hydrophilic catalyst part the following procedure has

\* Corresponding author. Tel.: +49 711 2572483; fax: +49 711 3052112847.  
E-mail address: [michael.lebert@daimler.com](mailto:michael.lebert@daimler.com) (M. Lebert).

been applied: half of the sonicated SWNT solution was mixed with a 60 wt% PTFE dispersion (Sigma–Aldrich®) at a ratio of 2:3. The SWNT/PTFE solution was filtered through a PC filter membrane ( $A = 5 \text{ cm}^2$ , pore size:  $0.1 \mu\text{m}$ ), using a simple filter flask and moderate vacuum. The SWNTs and the PTFE particles form an entangled hydrophobic network, which serves as the hydrophobic part of the GDE. Afterwards, the rest of the SWNT solution was filtered/deposited on top of the network creating the hydrophilic layer. This way, a micro-sized two-component material with a confined hydrophobic and hydrophilic part has been achieved. After washing thoroughly with water, the catalyst solution ( $0.1 \text{ M H}_2\text{PtCl}_6$  in isopropanol) was cast on to the hydrophilic side. Then, the entire network was annealed at  $100^\circ\text{C}$  under  $\text{H}_2$  flow for 1 h to reduce the precursor to metallic Pt. For MEA preparation a PC filter membrane (pore size  $10 \text{ nm}$ ) soaked with  $\text{H}_3\text{PO}_4$  was sandwiched between two of the electrodes described above.

For fuel cell testing, the SWNT electrodes are installed in a home-built cell holder with meander flow fields and an effective electrode area of  $3 \text{ cm}^2$ . The SWNT-GDEs were pressed with the hydrophobic side onto the flow fields, the hydrophilic side to the membrane.  $I$ – $V$  curves were taken at atmospheric pressure with non-humidified gases as a function of temperature.

### 2.1.2. Spray-dried MWNT electrodes

Spray-dried CNT electrodes have been prepared by depositing MWNT/Pt inks with defined Pt/C ratios by an air-brush onto polymer electrolyte membranes (Nafion 117). The membrane was heated to  $100^\circ\text{C}$  to improve the contact between membrane and catalyst.

The MWNTs were wet chemically platinized as described in detail in [13]. Electrodes of different thicknesses (e.g.  $1$  and  $6 \mu\text{m}$ ) were prepared from the same ink for performance tests at reduced Pt loading. In case of the  $1 \mu\text{m}$  sample only 1/6 of the liquid ink was deposited. Hence, as the density of Pt (number of Pt particles per  $\text{cm}^3$  carbon support) was kept constant the overall number of catalyst particles was reduced to 1/6.

Fuel cell tests of the spray-dried MWNT-MEAs were carried out in the same arrangement as described above, solely the active cell area was changed ( $A = 10 \text{ cm}^2$ ). The cells were operated at  $80^\circ\text{C}$  with humidified  $\text{H}_2$  and  $\text{O}_2$  ( $75\% < \text{r.h.} < 95\%$ ) to minimize ohmic losses of the electrolyte.

### 2.1.3. Control of catalyst composition

The efficiency of the catalyst preparation has been checked by X-ray fluorescence (XRF) after reduction of the hexachloroplatinate precursor and washing of the samples. No traces of Pt could be found in the (vaporized) filtrate indicating complete conversion of  $\text{Pt}^{4+}$  to metallic Pt and strong adherence of Pt to the CNT surface. Carbon loss also appears negligibly small, since no colour change of the filtrate was observed (already a few  $\mu\text{g}$  of CNTs would cause visible changes).

## 2.2. Aligned MWNTs for fuel cell electrodes

### 2.2.1. Partly aligned MWNTs on commercial carbon fibres

Partly aligned MWNTs on C-fibre substrates (carbon cloth, E-TEK® Co., USA) have been obtained by catalysed chemical vapour deposition (CCVD) in a  $2''$  tube furnace (Carbolite®). The MWNTs are grown on the graphitic fibre supports from thermally evaporated Fe catalyst with a thickness of  $0.7 \text{ nm}$  on top of a sputtered  $\text{Al}_2\text{O}_3$  ( $10 \text{ nm}$ ) support layer. The samples are heated in Ar flow of  $1 \text{ l/min}$  with a ramp rate of  $20^\circ\text{C/min}$ . The samples are annealed at  $750^\circ\text{C}$  in Ar/ $\text{H}_2$  atmosphere for 15 min to split the Fe film into nano-islands and catalysing the MWNT growth while feeding  $\text{C}_2\text{H}_2$  for 10 min.

### 2.2.2. Fully aligned and polymer stabilized MWNTs

For growth of fully aligned MWNTs a Si wafer has been coated with a  $10\text{-nm}$  thick Fe film and exposed at  $800^\circ\text{C}$  to  $\text{NH}_3$  (4 min) and to  $\text{C}_2\text{H}_2$  (10 min) at  $1.8 \text{ mbar}$ . Vapour deposition of parylene-N [14] was used to mechanically stabilize the fragile MWNT structure. The MWNT/parylene film was then removed from the silicon substrate by etching in  $30 \text{ wt}\%$  KOH solution at  $80\text{--}100^\circ\text{C}$  (etching results in HF are similar [15]). After a few minutes the composite film separates from the substrate leaving a flexible and stable film. Plasma oxidation was then performed to remove excess parylene [16]. Uncovering of the MWNTs is necessary to allow good electrical contact transport of (humidified) gases through the tubes [17].

## 3. Results and discussion

### 3.1. Thin film integrated SWNT electrodes

The preparation technique described above allows a flexible electrode architecture since desired functionalities can be introduced sequentially. This is shown by the layered structure of the GDE in Fig. 1b. The monolithic thin film electrode comprises the hydrophobic GDL (Fig. 1a) and the hydrophilic catalyst layer (Fig. 1c). The GDL part exhibits high porosity which is crucial for efficient gas supply and removal of product water. The corresponding TEM image shows the interpenetrating network of nano-sized SWNT bundles ('SWNT' in Fig. 1a) and micro-sized PTFE ('Teflon', Fig. 1a). The white arrows indicate interfaces between the hydrophobic and hydrophilic components. The morphology of the catalyst part (Fig. 1c) corresponds to bundles of platinized SWNTs (dark dots).

As shown by the TEM images in Fig. 2 the catalyst (dark spots) is distributed homogeneously in the CNT network. For statistical evaluation different sample regions (red circles Fig. 2a,b) were chosen to determine catalyst size and distribution (Fig. 2b). Fig. 2c displays the structure of the catalyst layer comprising open tube ends (x), aligned tubes (y) and Pt particles (z).

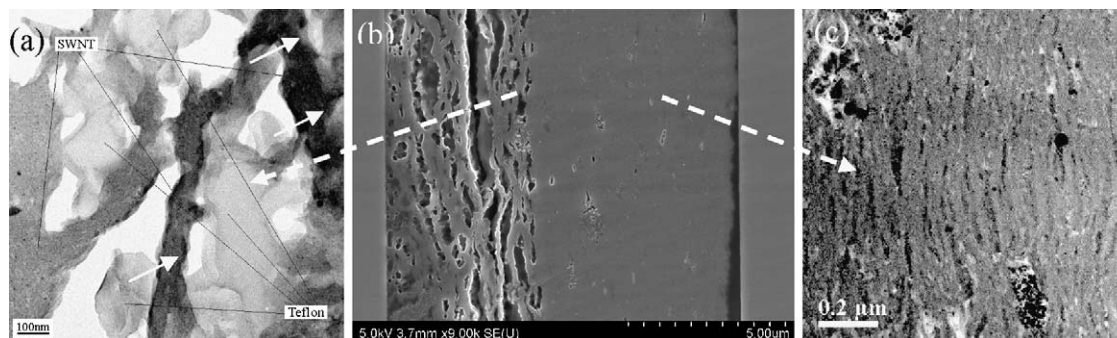


Fig. 1. (a) SWNT/PTFE-gas diffusion layer (TEM), (b) cross-section of integrated SWNT electrode (SEM), and (c) SWNT/Pt catalyst layer (TEM).

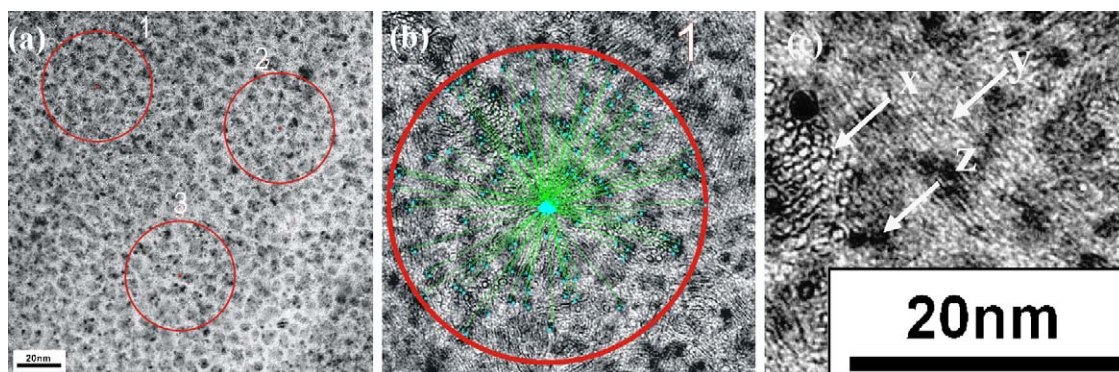


Fig. 2. TEM images of catalyst layer: (a) statistical evaluation, (b) size/distance identification, and (c) enlarged structure details.

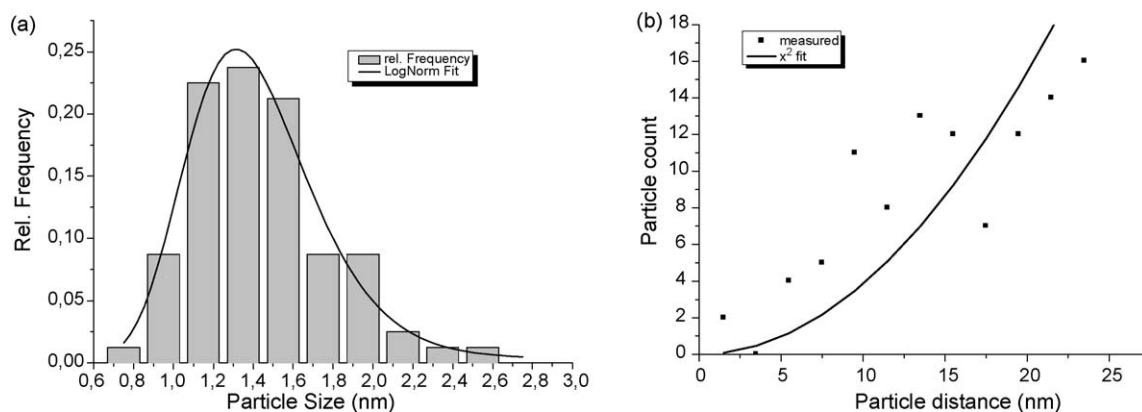


Fig. 3. (a) Size distribution and (b) density distribution of Pt catalyst.

The Pt particles with an average size of 1.4 nm (Fig. 3a) are appropriate for the catalytic reactions at anode and cathode although their size is smaller than the optimum size of 3–4 nm [18]. The observed increase of the Pt amount with spherical extension indicates homogeneous catalyst distribution (Fig. 3b). The quadratic growth fit in Fig. 3b is drawn as a guideline for the eye.

### 3.2. Performance of the SWNT-electrode at elevated temperature

The performance of these novel SWNT-electrodes and of commercial amorphous carbon electrodes (E-TEK) is compared

in Fig. 4a. Fig. 4b presents the comparison with conventional PAFCs.

Power densities at 125 °C differ only slightly (Fig. 4a) indicating that none of the carbon materials has a distinct advantage. This suggests that the catalyst-support interaction is quite similar for the different forms of carbon. Fig. 4b compares the SWNT cell (SWNT-PAFC) with the conventional PAFC and the high temperature-PEMFC (HT-PEMFC) at atmospheric pressure and similar loading (0.5 mg Pt cm<sup>-2</sup>).

A direct comparison of the SWNT-PAFC with these FCs is restricted by the limited thermal stability of PC (glass temperature

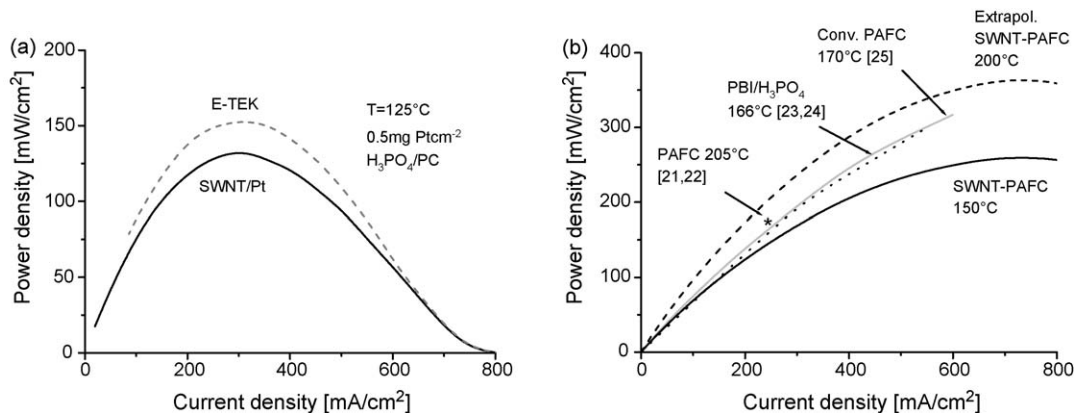


Fig. 4. PAFC performance: (a) E-TEK vs. SWNT electrode and (b) SWNT- vs. conventional PAFCs.



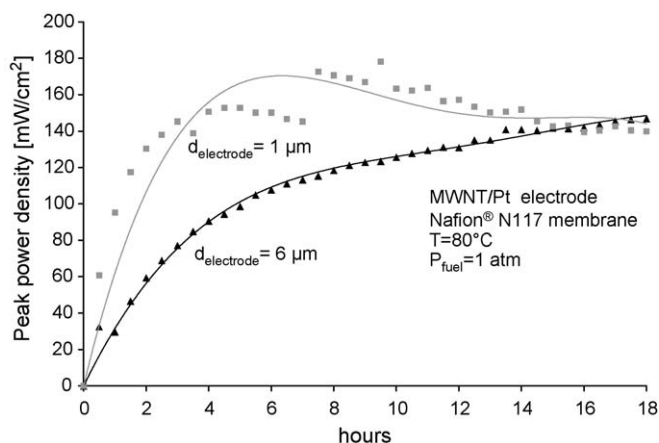


Fig. 5. PEFC performance (low catalyst loading).

<150 °C [19]). However, one may safely estimate the upper performance limit of the SWNT-PAFC at 200 °C by taking the power density change due to the altered IR loss of the electrolyte (main loss factor in the intermediate region of a fuel cell  $I$ - $V$  curve) into account. The extrapolated curve fits into the literature data: at a typical current density of  $0.24 \text{ A cm}^{-2}$  as PAFC operating point [20]) the corresponding power density is close to  $0.2 \text{ W cm}^{-2}$  which is slightly higher than the best value for the PAFC ( $0.18 \text{ W cm}^{-2}$  at 205 °C marked as \* in Fig. 4b [21]). The SWNT-PAFC results also agree with those of recent HT-PEMFCs such as PBI/ $\text{H}_3\text{PO}_4$  [22,23] (dotted line in Fig. 4b) and conventional PAFCs [24]. Evidently, the thin film SWNT-PAFC is competitive with the well-established PAFC and HT-PEMFC. The potential of SWNT electrodes becomes obvious when comparing some of their basic properties (Table 1) with those of amorphous carbon electrodes: mass and thickness are reduced by more than one, conductivity by 2–3 orders of magnitude.

### 3.3. Performance of spray-dried MWNT electrode with reduced catalysed loading

Fig. 5 presents the power densities of two Nafion 117-based fuel cells where MWNT have been sprayed directly onto the membrane. Electrodes of two different thicknesses but identical catalyst densities have been prepared. This way, the catalyst loading was lowered from  $0.3 \text{ mg Pt/cm}^2$  ( $6\text{-}\mu\text{m}$  electrode thickness) to  $0.05 \text{ mg Pt/cm}^2$  ( $1\text{-}\mu\text{m}$  electrode thickness). All other parameters

Table 1

Properties of SWNT- and conventional carbon electrode (E-TEK).

	$d$ ( $\mu\text{m}$ )	$m$ ( $\text{mg/cm}^2$ )	$\sigma^a$ (S/cm)
SWNT	$\sim 10$	$\sim 0.7$	$160^b\text{--}2500^c$
E-TEK [25]	$\sim 400$	$\sim 21$	$\sim 0.6$

<sup>a</sup> At room temperature.

<sup>b</sup> Sonication in SDS.

<sup>c</sup> Sonication in conc. nitric acid.

of the fuel cell experiment have been kept constant. Fig. 5 shows the change of power density during cell operation.

The power densities of both MEAs stabilize after 14 h of cell operation. Both MEAs show a similar value ( $140 \text{ mW/cm}^2$ ) indicating that a substantial part of the catalyst in the thicker sample is ineffective. Assuming that mainly the catalyst particles in direct contact with the electrolyte surface are performance limiting, a rather thin layer of Pt would be sufficient. The thickness of the catalytic active interface layer will be restricted to the diffusion length of  $\text{H}^+$ , if this species determines the reactions. This leads to the conclusion that the CNT based MEA architecture has a distinct saving potential in terms of mass-, volume and catalyst.

### 3.4. Electrodes using aligned carbon nanotubes

Here, we introduce electrode architectures based on aligned MWNT structures. Fuel cell testing has not been carried out yet and is part of ongoing future work.

Fig. 5a depicts a carbon fibre with  $d \sim 20 \mu\text{m}$  densely covered by MWNTs with  $d \sim 40 \text{ nm}$  (see Fig. 6a and b). According to initial BET measurements the surface area is enhanced with respect to the fibre area by a factor  $4 \pm 1$ . This would not only increase the 3-phase contacts but also allow the deposition of higher amounts of catalyst leading to an increased fuel cell performance.

The fully aligned MWNTs shown in Fig. 6c present a kind of model system. Notably the dimensions (thickness and structure) can be controlled by the deposition process of the growth catalyst (structure) and the growth parameters (CNT length or electrode thickness, respectively). The rather fragile structure can be stabilized by imbedding the entire structure in a polymer matrix. Vapour deposition of Parylene N and subsequent plasma etching of excess polymer material to uncover the tips of the MWNTs proved to be a suitable method. Fig. 6c shows a SEM image of such a MWNT forest imbedded in Parylene N. Whether these ordered nanostructures are more advantageous than the randomly oriented ones has to be verified by forthcoming experiments.

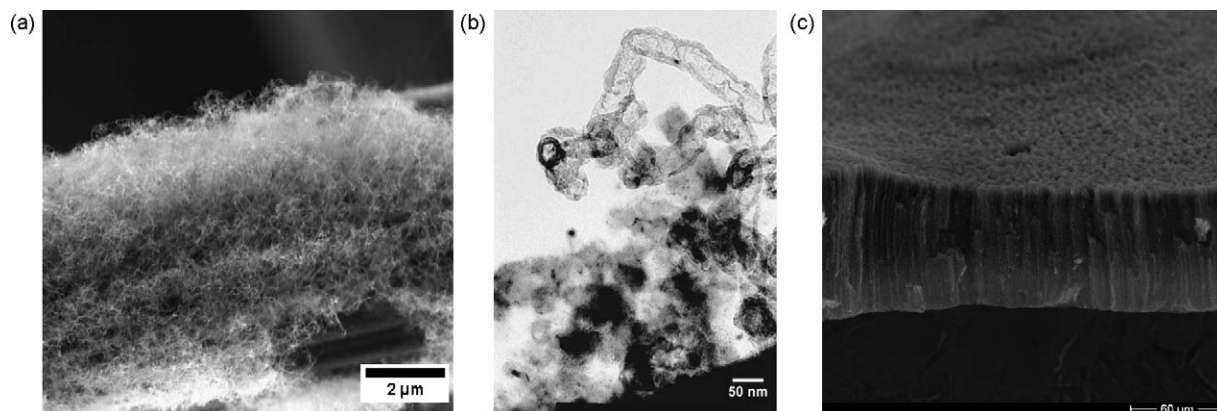


Fig. 6. (a) Partly aligned MWNTs on a carbon fibre (SEM), (b) magnification (TEM), and (c) aligned MWNTs imbedded in Parylene N (SEM).

#### 4. Conclusions

The liquid state processing of CNT networks allows flexible electrode design and opens new ways for significantly mass-/volume-reduced fuel cell electrodes (MEAs) for low and intermediate temperature fuel cells. CNT network electrodes deposited directly onto a Nafion membrane have a high saving potential, since the electrode thickness can be distinctly reduced at constant CNT/catalyst ratio, i.e. comparable performance is obtained at reduced catalyst loading. This method is also suitable for an automatised and controlled deposition process which would also lead to an optimized structure in terms of thickness reduction/catalyst saving. With respect to technical shortcomings, the most important applications are light weight and micro-sized high performance power supplies and battery chargers for consumer electronics such as portable devices.

#### Acknowledgements

The authors like to thank D. Su and co-workers from the Fritz-Haber-Institute of the Max-Planck-Society (Berlin) for TEM/SEM recordings, G.S. Duesberg from CRANN/Trinity College Dublin for providing aligned MWNTs and G. Ulbricht from the Max-Planck-Institute for Solid State Research (Stuttgart) for coating the MWNTs with parylene. Financial support by the EU project CANAPE (Contract No. 500096) is gratefully acknowledged.

#### References

- [1] D.J. Guo, H.L. Li, J. Electroanal. Chem. 573 (2004) 197.
- [2] X. Wang, W. Li, Z. Chen, M. Waje, Y. Yan, J. Power Source 158 (2006) 154.
- [3] C.H. Wang, H.Y. Du, Y.T. Tsai, C.P. Chen, C.J. Huang, L.C. Chen, K.H. Chen, H.C. Shih, J. Power Source 171 (2007) 55.
- [4] M. Wienecke, M.C. Bunesco, M. Pietrzak, K. Deistung, P. Fedtke, Synth. Met. 138 (2003) 165.
- [5] Fleckner, et al., United States Patent, US 6,589,682 B1 (2003).
- [6] K.K.S. Lau, J. Bico, K.B.K. Teo, M. Chhowalla, G.A.J. Amaratunga, W.I. Milne, G.H. McKinley, K.K. Gleason, Nano Lett. 3 (12) (2003) 1701.
- [7] E. Frackowiak, G. Lota, T. Cacciaguerra, F. Béguin, Electrochem. Commun. 8 (2005) 129.
- [8] W. Li, C. Liang, W. Zhou, H. Han, Z. Wei, G. Sun, Q. Xin, Carbon 40 (2002) 787.
- [9] M. Cinke, J. Li, B. Chen, A. Cassell, L. Delzeit, J. Han, M. Meyyappan, Chem. Phys. Lett. 365 (2002) 69.
- [10] P. Nikolaev, M.J. Bronikowski, R.K. Bradley, F. Rohmund, D.T. Colbert, K.A. Smith, R.E. Smalley, Chem. Phys. Lett. 313 (1999) 91.
- [11] M. Kaempgen, M. Lebert, M. Haluska, N. Nicoloso, S. Roth, Adv. Mater. 20 (2008) 616.
- [12] Y. Liu, J. Chen, W. Zhang, Z. Ma, G.F. Swiegers, C.O. Too, G.G. Wallace, Chem. Mater. 20 (8) (2008) 2603.
- [13] M. Soehn, M. Lebert, T. Wirth, S. Hofmann, N. Nicoloso, J. Power Source 176 (2008) 494.
- [14] R.R.A. Callahan, G.B. Raupp, S.P. Beaudoin, J. Vac. Sci. Technol. B 19 (3) (2001) 725.
- [15] B.J. Hinds, N. Chopra, T. Rantell, R. Andrews, V. Gavalas, L.G. Bachas, Science 303 (2004) 62.
- [16] R.D. Tacito, C. Steinbrüchel, J. Electrochem. Soc. 143 (1996) 1974.
- [17] J.K. Holt, H.G. Park, Y. Wang, M. Stadermann, A.B. Artyukhin, C.P. Grigoropoulos, A. Noy, O. Bakajin, Science 312 (2006) 1034.
- [18] M. Peuckert, T. Yoneda, R.A. Dalla Betta, M. Boudart, J. Electrochem. Soc. 133 (1986) 944.
- [19] W. Schröter, K.-H. Lautenschläger, H. Bibrack, A. Schnabel, Chemie, VEB Fachbuchverlag, Leipzig, 1986.
- [20] I. Staffel <[http://www.fuelcells.bham.ac.uk/documents/Review\\_of\\_PAFC.pdf](http://www.fuelcells.bham.ac.uk/documents/Review_of_PAFC.pdf)>.
- [21] U.S. Department of Energy, Fuel Cell Handbook, fifth edition, DE-AM26-99FT 40575, 2000.
- [22] Q. Li, J.O. Jensen, C. Pan, V. Bandur, M.S. Nilsson, F. Schönberger, A. Chromik, M. Hein, T. Häring, J. Kerres, N.J. Bjerrum, Fuel Cells 3–4 (2008) 188.
- [23] C. Henschel, Fuel Cells Bulletin 2 (2006) 12.
- [24] K.H. Yoon, J.Y. Choi, J.H. Jang, Y.S. Cho, K.H. Jo, J. Appl. Electrochem. 30 (2000) 121.
- [25] E-TEK, Gas Diffusion Electrode: Catalyzed ELAT, technical product information, 2003.